

Published in final edited form as:

Nat Struct Mol Biol. 2015 August ; 22(8): 597–602. doi:10.1038/nsmb.3052.

Structural basis for the RING catalyzed synthesis of K63 linked ubiquitin chains

Emma Branigan¹, Anna Plechanovová¹, Ellis Jaffray¹, James H. Naismith², and Ronald T. Hay¹

¹Centre for Gene Regulation and Expression, University of Dundee, Dundee, United Kingdom

²Biomedical Sciences Research Complex, University of St Andrews, St Andrews, United Kingdom

Abstract

The RING E3 ligase catalysed formation of lysine 63 linked ubiquitin chains by the Ube2V2–Ubc13 E2 complex is required for many important biological processes. Here we report the structure of the RING domain dimer of rat RNF4 in complex with a human Ubc13~Ub conjugate and Ube2V2. The structure has captured Ube2V2 bound to the acceptor (priming) ubiquitin with Lys63 in a position that could lead to attack on the linkage between the donor (second) ubiquitin and Ubc13 that is held in the active “folded back” conformation by the RING domain of RNF4. The interfaces identified in the structure were verified by *in vitro* ubiquitination assays of site directed mutants. This represents the first view of the synthesis of Lys63 linked ubiquitin chains in which both substrate ubiquitin and ubiquitin-loaded E2 are juxtaposed to allow E3 ligase mediated catalysis.

INTRODUCTION

Ubiquitin is a flexible and reversible signal that serves to alter the fate of the protein to which it is conjugated. Modification by ubiquitin is mediated by an enzymatic cascade in which ubiquitin is initially linked via a thioester bond to one of two ubiquitin activating enzymes. The ubiquitin then undergoes a transthiolation reaction onto one of about 40 different ubiquitin conjugating enzymes (E2s) which then interact with one of the 600 substrate specific ubiquitin E3 ligases^{1,2}. RING E3 ligases prime the ubiquitin loaded E2 for catalysis by a mechanism of conformational selection in which RING residues contact both the E2 and donor ubiquitin, immobilising the ubiquitin and locking its C-terminus into a groove on the E2³⁻⁵. It is thought that immobilising the donor ubiquitin onto the E2 will orientate the thioester between ubiquitin and the E2 in an optimal orientation to undergo

Users may view, print, copy, and download text and data-mine the content in such documents, for the purposes of academic research, subject always to the full Conditions of use:http://www.nature.com/authors/editorial_policies/license.html#terms

Correspondence and requests for materials should be addressed to R.T.H. (R.T.Hay@dundee.ac.uk) or J.H.N. (naismith@st-andrews.ac.uk).

Author Contributions E.B. cloned, expressed and purified proteins, carried out structural analysis, conducted biochemical experiments and interpreted the data. A.P. cloned, expressed and purified proteins, conducted biochemical experiments and interpreted the data. E.G.J. purified recombinant proteins and carried out biochemical analysis. J.H.N. contributed to structural analysis and data analysis. E.B., A.P., J.H.N. and R.T.H. wrote the paper. R.T.H. conceived the project and contributed to data analysis.

Accession Codes: Coordinates and structure factors of the Ubc13~Ub–Ube2V2–RNF4 RING and Ubc13~Ub–RNF4 RING structures were deposited in the Protein Data Bank under accession codes 5AIT and 5AIU respectively.

nucleophilic attack by the ϵ -amino group of a lysine in the substrate⁶. If the attacking lysine residue is from another molecule of ubiquitin then this will result in the formation of an isopeptide bond between two ubiquitin molecules and if repeated multiple times will result in the generation of a ubiquitin chain. Ubiquitin contains 7 lysine residues and all, along with the N-terminal amino group of ubiquitin, can be utilised to form the 8 different di-ubiquitin species.

We had previously shown that the SUMO Targeted Ubiquitin E3 Ligase (STUbL) RNF4 was responsible for the UbcH5A catalysed formation of K48 chains that targeted SUMO modified PML protein for proteasomal degradation in response to arsenic treatment⁷. It is also involved in the mammalian DNA damage response, facilitating DNA repair⁸⁻¹¹. SUMO chains bind SUMO interaction motifs of RNF4 inducing dimerization of the RING domain, which is required for its function as an E3 ligase¹². Thus, RNF4 is recruited to DNA damage sites by recognition of SUMO-modified DNA damage associated proteins such as MDC1 where it is responsible for the formation of K63 linked ubiquitin chains that are involved in signaling DNA damage repair¹¹. K63 linked ubiquitin chains are synthesised by the E2 enzyme Ubc13, but only when it is complexed with UEV (Ube2V1 and Ube2V2 in humans and MMS2 in yeast), a pseudo E2¹³ that serves to orientate the acceptor ubiquitin such that the K63 can attack the thioester linking the donor ubiquitin to Ubc13¹⁴. In the case of K63 chain formation the substrate is an acceptor ubiquitin that is positioned by UEV, but as yet there are not structures available of an acceptor ubiquitin that is poised to attack the thioester of a donor ubiquitin held in place by an activating ubiquitin E3 ligase. To address this question we have determined a structure of the RING domain dimer of RNF4 in complex with a Ubc13~Ub conjugate and Ube2V2. The structure has captured K63 in the acceptor ubiquitin in a position that could lead to attack on the active site of Ubc13 that is linked to the donor ubiquitin. Biochemical analysis suggests that in addition to positioning the acceptor ubiquitin Ube2V2 is also required for RNF4 mediated activation of the Ubc13~Ub thioester.

RESULTS

RNF4 dependent synthesis of K63 chains by Ube2V2 and Ubc13

We had previously shown that in response to DNA damage the STUbL RNF4 (Fig. 1a) was responsible for the formation of K63 linked ubiquitin chains¹¹. We therefore tested the ability of RNF4, Ubc13 and Ube2V2 to catalyse K63 chain synthesis on a ubiquitin-primed tetraSUMO substrate (Fig. 1a). Ubc13 combined with Ube2V2 efficiently generated K63 chains linked to ubiquitin-primed tetraSUMO substrate in the presence of RNF4¹⁵ but crucially Ubc13 alone is inactive even in the presence of RNF4 (Fig. 1b). In the absence of substrate a low level of unanchored K63 chains were generated (Fig. 1b) and, as visualised by Western blotting (Supplementary Fig. 1a) K63 chain synthesis was stimulated by the presence of tetraSUMO lacking the N-terminal ubiquitin although tetraSUMO itself was not a substrate for ubiquitin modification. This is consistent with SUMO chain-induced dimerization as a mechanism for RNF4 activation¹² and for the requirement of a ubiquitin-modified (also known as priming) substrate.

Structure of Ubc13~ubiquitin–Ube2V2–RNF4 RING complex

To establish the molecular basis of the RNF4 catalysed synthesis of K63 chains by Ube2V2–Ubc13 we determined structures of ubiquitin-loaded Ubc13 (Ubc13~Ub) in complex with the RING domain of RNF4 in the presence (Fig. 2a) and in the absence (Fig. 2b) of Ube2V2 (Table 1). We used a stable isopeptide linked E2~Ub to mimic the unstable thioester⁴ (Supplementary Fig. 1b–e). The Ubc13~Ub–RNF4 RING structure closely resembles that described previously for UbcH5A~Ub–RNF4 RING⁴ (Supplementary Fig. 2a). In these complexes the RNF4 RING dimer sits at the centre with a two-fold rotational axis of symmetry relating the RNF4 RING domains. The Ubc13~Ub–Ube2V2–RNF4 structure (Fig. 2a) lacks the two-fold symmetry of the Ubc13~Ub–RNF4 RING and UbcH5A~Ub–RNF4 RING complexes, therefore we discuss each “half” split at the RNF4 RING domains separately. In one half the Ubc13~Ub conjugate is bound to the RING domain, as seen in the Ubc13~Ub–RNF4 RING structure (Supplementary Fig. 2b) and a Ube2V2 is bound to Ubc13 engaging the surface opposite to that docked to the RING. In the other half of the structure, the RING, Ubc13 and Ube2V2 adopt the same configuration as described above however ubiquitin is found in an unexpected location. In the asymmetric unit one of the ubiquitin molecules tethered by the isopeptide bond to the E2, appears to project away from the complex (Fig. 2a). However analysis of packing of the molecules in the crystal reveals the reason for the displaced ubiquitin; it makes extensive contacts with a symmetry related Ube2V2 molecule and thus mimics the priming (substrate-bound) ubiquitin (Fig. 2c and Supplementary Fig. 3a).

By selecting a different symmetry related ubiquitin within the Ubc13~Ub–Ube2V2–RNF4 RING crystal structure, a model that has captured Ube2V2 bound to the acceptor ubiquitin can be created. The donor ubiquitin is held in the activated “folded back” conformation by the RING domain of RNF4 seen previously⁴, while the acceptor ubiquitin is oriented by Ube2V2 such that its K63 is in a position that could lead to attack the thioester linkage between the donor ubiquitin and Ubc13 (Supplementary Fig. 3b–e). In the present structure the ϵ -amino group of K63 is 12.5 Å from the active site of Ubc13, but relatively minor adjustments of the components of the complex could bring the lysine residue into a position where it would be close enough to carry out nucleophilic attack on the thioester between ubiquitin and Ubc13. This arrangement in the crystal is thus a structural model for all components required to transfer a ubiquitin onto Lys63 of another ubiquitin molecule; the first step in the synthesis of K63 chains (Fig. 2d).

Validation of the Ubc13~Ub–Ube2V2–RNF4 RING structure

The validity of this model is supported by an analysis of the individual protein-protein interfaces. The interfaces between E3 ligase and E2~Ub, between ubiquitin and the pseudo E2 and between Ubc13 and the pseudo E2 have been observed previously^{3-5,14,16-22} (Supplementary Fig. 4a–c). To probe the key interfaces (Fig. 3a–e) mutations were introduced into Ube2V2 and Ubc13 and the modified proteins assayed. Ube2V2 F13 contacts Ubc13 (Fig. 3b) and Ube2V2 F13A, which was previously shown to perturb binding to Ubc13 in yeast²¹, is almost completely inactive in ubiquitination (Fig. 3f). Ube2V2 S32 forms a hydrogen bond with the backbone of the acceptor ubiquitin G47 (Fig. 3a), and the importance of this residue in acceptor ubiquitin binding¹⁴ is consistent with the

loss of activity of Ube2V2 S32A in ubiquitination (Fig. 3f) although there is almost no difference in the affinity for Ubc13 (Supplementary Fig. 5a, b).

The C-terminus of the donor ubiquitin is locked down in the active site groove of Ubc13 (Fig. 3c) by RNF4. This appears to be a conserved arrangement for activation of the thioester between ubiquitin and ubiquitin-like proteins and their cognate E2s^{3-5,23,24} and was evident in the UbcH5A~Ub~RNF4 RING structure⁴. A hydrogen bond between the backbone of ubiquitin R74 and the side chain of D87 in UbcH5A was identified as critical as was D117 that was predicted to be involved in deprotonating and/or positioning the incoming lysine^{4,25}. Equivalent mutations in Ubc13 (D89A, D119A) were also inactive (Fig. 3c, f), as were mutations disrupting interactions between the donor ubiquitin and Ubc13 (L106A) and between Ubc13 (R7A and M64A) and RNF4 (Fig. 3 d–f). This suggests that RNF4 plays a similar role in Ubc13 catalysis by activating the thioester bond.

Activation of Ubc13~Ub thioester by Ube2V2 and the RNF4 RING

To establish the requirements for activation of the Ubc13~Ub thioester we carried out lysine discharge assays (the amino acid lysine acts as the substrate) on ubiquitin-loaded Ubc13 (Fig. 4a–c). This eliminates any role of substrate in recognition and reports on the activation of the ubiquitin~E2 thioester bond. Unexpectedly, neither RNF4 nor a constitutively active RNF4 fused to a second RNF4 RING domain (RNF4-RING, Fig. 4a) alone were able to substantially activate ubiquitin discharge from the Ubc13~ubiquitin conjugate. However, when both RNF4-RING and Ube2V2 were present the rate of ubiquitin discharge was dramatically increased. RNF4-RING was required as Ube2V2 alone had only a small effect on the rate of ubiquitin discharge. Binding of ubiquitin to Ube2V2 does not have a substantial impact on RNF4-mediated ubiquitin discharge from Ubc13 as Ube2V2 S32A that perturbs ubiquitin binding has almost wild-type activity (Fig 4b, c).

We conclude that Ube2V2 and RNF4 together induce an active conformation of the Ubc13~Ub thioester. However, we do not identify any obvious structural changes at the E2 catalytic site that could explain the requirement for Ube2V2 in RNF4 mediated Ubc13~Ub activation when comparing the Ubc13~Ub~RNF4 RING complexes with and without Ube2V2 (Supplementary Fig. 2b). Moreover, the Ubc13~Ub~RNF4 RING structure is very similar to that of the catalytically active UbcH5A~Ub~RNF4 RING (Supplementary Fig. 2a). We note that our structures are isopeptide- rather than thioester-linked Ubc13~Ub conjugates and whilst simple modelling of the thioester does not reveal any change in the structure at the active site, the occurrence of subtle changes that could influence catalysis cannot be excluded.

A key region in Ubc13 that is contacted by Ube2V2 is the D81 to R85 loop that is directly connected to the loop that includes the catalytic cysteine (K87 in our structures) and to N79, a catalytically important residue that is thought to stabilise the tetrahedral intermediate and support the active site loop^{26,27}. The loop D81 to R85 of Ubc13 makes a number of contacts with Ube2V2, including a salt bridge between R85 of Ubc13 and E20 of Ube2V2 (Fig. 3c, Supplementary Fig. 6a, b). In testing the importance of this salt bridge, Ubc13 R85S and R85E mutants were shown to have dramatically reduced catalytic activity but Ube2V2 E20A and E20R were fully active (Fig. 3f, Supplementary Fig. 6c). Moreover, a charge

swap combination of Ubc13 R85E and Ube2V2 E20R did not rescue activity (Supplementary Fig. 6c). This suggests that Ubc13 R85 has a critical role in maintaining the active site in an optimal conformation for catalysis, but this is not dependent on the salt bridge between Ubc13 R85 and Ube2V2 E20. The sequence of the D81 to R85 loop varies between different E2 enzymes (Supplementary Fig. 6d). Ubc13 D81 can make several hydrogen bonds with the backbone of this loop and a salt bridge with R85 (Fig. 3c). In UbcH5A, N79 can make similar hydrogen bonds but as the equivalent residue of R85 in Ubc13 is S83 in UbcH5A there is no salt bridge (Supplementary 6a, b). Mutation D81A in yeast Ubc13 decreased the amount of di-ubiquitin formed compared to wild-type²¹. We could not express human Ubc13 D81A but Ubc13 D81N which preserves the hydrogen bonds with the loop backbone, had only modestly reduced activity (Supplementary Fig. 6c). Introduction of the R85S mutation into wild-type Ubc13 reduces activity dramatically (Fig. 3f). This mutation not only removes the electrostatic interactions with Ubc13 D81 and Ube2V2 E20, but is predicted to disrupt a number of hydrophobic interactions (Fig. 3b and Supplementary Fig. 6a). Ubc13 R85S increases the K_d for Ube2V2 by more than 30 times, while Ube2V2 E20A results in an increase of 4 times in the K_d for WT Ubc13 (Supplementary Fig. 5a, b). However introduction of R85S in Ubc13 D81N is almost without consequence compared to Ubc13 D81N (Supplementary Fig. 6c). Thus it appears that R85 is essential only when the negatively charged D81 is present. We suggest that Ubc13 activation by Ube2V2 results from a change in the conformation or immobilisation of the R85–D81 interaction upon Ube2V2 binding which induces the catalytic configuration of the active site loop.

DISCUSSION

The structure we have determined is a model for the first step in the synthesis of polyubiquitin chains (Fig. 4d): that is the transfer of a donor ubiquitin from its E2 thioester conjugate to the K63 of the priming ubiquitin. To obtain this structure it was necessary to replace the reactive thioester between ubiquitin and Ubc13 by a stable isopeptide bond. Modelling the thioester in place of the isopeptide linkage and modifying the rotamer of the side chain of K63 of the acceptor ubiquitin (which is not well defined in the electron density maps, Supplementary Fig. 3b, c) brings K63 of the acceptor ubiquitin to within 9 Å of the carbonyl carbon of the thioester linkage. Crystal packing allowed us to capture the acceptor ubiquitin in the structure but the distortion from perfect nucleophilic attack geometry expected in solution may arise from both crystal packing and tethering of the ubiquitin to a Ubc13 molecule. In this situation the Ubc13–Ube2V2 interaction would dominate as this is a much higher affinity interaction (50 nM) than the Ub–Ube2V2 interaction (30 μM)¹⁷. However a simple rigid body rotation of the ubiquitin by a few degrees or change in the precise position of a RING domain could reduce the distance to within the range of nucleophilic attack. The value of the structure is that it has captured Ube2V2 bound to the acceptor ubiquitin with Lys63 in a position that could lead to attack on the linkage between the donor ubiquitin and Ubc13 that is held in the active “folded back” conformation by the RING domain of RNF4. This allowed us to build a model for the RING mediated formation of K63 chains that was tested by mutagenesis and biochemical analysis. The arrangement in the active site is similar to that observed for the RBX1–Ubc12~NEDD8–Cul1–DCN1

complex where the NEDD8 is “folded back” onto the E2, but where modeled lysine of the substrate, unaffected by crystal packing makes a much closer approach (2.6 Å) to the Ubc12~NEDD8 linkage²⁴.

Synthesis of K63 linked ubiquitin chains onto a target protein is at the heart of many cellular processes. The structure reveals that Ube2V2 regulates this process by binding and presenting the priming ubiquitin such that its K63 attacks the thioester linkage between the donor ubiquitin and Ubc13 (to which Ube2V2 also binds). Our data show that in the presence of RNF4 Ube2V2 has an additional role in increasing the reactivity of the Ubc13~Ub thioester linkage. Without Ube2V2, Ubc13 cannot efficiently transfer ubiquitin to any substrate. Thus only when Ube2V2 is bound and ubiquitin is presented in the correct spatial orientation is Ubc13 activated. Such exquisite and multilayered control is emerging as a common feature of ubiquitin²⁸ and ubiquitin-like^{23,24} modification systems.

Methods

Cloning, expression and purification of recombinant proteins

Rattus norvegicus RNF4 and linear fusions, RING-RING and RNF4-RING, were expressed and purified as described previously for WT RNF4²⁹. A linear fusion of four SUMO-2 molecules (4xSUMO-2) and ubiquitin and four SUMO-2 molecules (Ub~4xSUMO-2) were expressed and purified as described previously^{15,29}. Human Ube2V2 was subcloned into the pLou3 vector using NcoI & BamHI restriction sites. Human Ubc13 (also known as UBE2N) was subcloned into the pHISTEV30a vector using NcoI & HindIII restriction sites. C87K and K92A were introduced into Ubc13 by site-directed mutagenesis. His₆-tagged Ubc13 and His₆-MBP-tagged Ube2V2 were purified by Ni-NTA (Qiagen) affinity chromatography. To cleave off the His₆-tag and His₆-MBP-tag, both proteins were incubated with TEV protease and dialyzed overnight into 50 mM Tris, 150 mM NaCl, 0.5 mM TCEP, pH 7.5. Any uncleaved protein, free His₆-tag or His₆-MBP-tag and TEV protease (also His₆-tagged) were removed by Ni-NTA affinity chromatography. Untagged Ubc13 and Ube2V2 were further purified by size exclusion chromatography using HiLoad Superdex 75 16/60 (GE Healthcare) and 20 mM Tris, 150 mM NaCl, 0.5 mM TCEP, pH 7.5 as running buffer. Cloning of Ubc13 and Ube2V2 yielded two extra residues (Gly-Ala) at the N-terminus of both proteins after cleavage with TEV protease.

Preparation of isopeptide linked Ubc13~Ub conjugate

Ubiquitin purified from bovine erythrocytes (U6253, Sigma-Aldrich) was used for conjugation to Ubc13 via an isopeptide linkage. A similar method was used to load ubiquitin onto the active site of Ubc13 as used previously for a UbcH5A~Ub conjugate⁴. Ubc13 (100 μM) and ubiquitin (120 μM) and His₆-Ube1 (0.8 μM) were incubated together at 37 °C for 21 hours in 50 mM Tris pH 10.0, 150 mM NaCl, 3 mM ATP, 5 mM MgCl₂ and 0.5 mM TCEP (Supplementary Fig. 1b). The isopeptide linked Ubc13~Ub conjugate was either purified directly or mixed in a 1:1 ratio with Ube2V2 and then purified by size exclusion chromatography on a HiLoad Superdex 75 16/60 (GE Healthcare) and 20 mM Tris, 150 mM NaCl, 0.5 mM TCEP, pH 7.5 as running buffer (Supplementary Fig. 1d).

Crystallization of Ube2V2-Ubc13-Ub-RNF4 RING

The Ube2V2-Ubc13-Ub complex was mixed in a 2:1 molar ratio with the RING-RING linear fusion in a buffer containing 20 mM Tris, 150 mM NaCl, 0.5 mM TCEP, pH 7.0 and concentrated to 10 mg ml⁻¹. Crystals of the complex were grown by sitting-drop vapour diffusion at 20 °C. 1.25 µl of protein was mixed with 1.25 µl of reservoir solution (16.7% (v/v) PEG MME 550, 0.1 M MES pH 7.0). Crystals appeared after a few hours and grew to their final size after 1 day. Crystals were cross-linked with glutaraldehyde for 30 minutes at 20 °C by placing 2 µl of glutaraldehyde in the bottom of a PCR tube and inserting it into the reservoir well. Glutaraldehyde was removed and crystals were then immediately soaked in 15% (v/v) glycerol, 16.7% (v/v) PEG MME 550, 0.1 M MES pH 7.0 and flash frozen in liquid N₂.

Crystallization of Ubc13-Ub-RNF4 RING

The Ubc13-Ub conjugate was mixed in a 2:1 molar ratio with the RING-RING linear fusion in a buffer containing 20 mM Tris, 150 mM NaCl, 0.5 mM TCEP, pH 7.0 and concentrated to 10 mg ml⁻¹. Crystals of the complex were grown by sitting-drop vapour diffusion at 20 °C. 0.2 µl of protein was mixed with 0.2 µl of reservoir solution (0.2 M MgCl₂, 0.1 M Tris pH 8.5, 20% (w/v) PEG 8000). Crystals appeared after 1 day and grew to their final size after 2 days. Crystals were soaked in a 2:1 ratio of reservoir solution and 100% ethylene glycol and flash frozen in liquid N₂.

Structure determination for Ube2V2-Ubc13-Ub-RNF4 RING and generation of the canonical model

The long cell edge of the crystals required us to pre-orient the crystals for data collection to avoid overlaps. The crystals varied in quality and we screened multiple crystals. We collected the data on beamline IO4 at Diamond (wavelength 0.9795 Å) at 100 K using 0.2 oscillations for 400 images before the diffraction deteriorated. The detector was positioned to ensure a clear separation of the spots rather than to maximize the resolution. Thus the highest resolution shell of data observed (3.49 to 3.4 Å) is incomplete, as it is located in the corners of the plate. The data in the next highest shell 3.58 to 3.49 Å were 99% complete. Data were indexed, integrated and scaled using XIA2, XDS and CCP4³⁰⁻³⁵. The structure was solved by molecular replacement using PHASER³⁶. The model was refined using REFMAC5³⁷ and evaluated using MolProbity³⁸. The final statistics are shown in Table 1. The coordinates and data are available at the RCSB with the accession code 5ait. The final model and electron density map for the donor and acceptor ubiquitin at position K63 is shown (Supplementary Fig. 3 b-e). Looking at the crystal packing reveals the reason why one of the ubiquitin molecules is displaced; in the new position the ubiquitin makes extensive contacts with a symmetry related Ube2V2 molecule (Supplementary Fig. 3a). If one transforms this ubiquitin by the crystallographic operator $-X+Y, -X, Z+1/3$ then what we term the 'canonical model' can be generated (Fig. 2c). The canonical structure interfaces bury 750 Å² more surface area than the original structure³⁹. Although we discuss the canonical model, it is important to note that it is 'artificial' and not found in solution. This is because the transformed ubiquitin is in reality covalently linked to Ubc13 (Chain E); the canonical model arises because of crystal packing.

Data collection and structure determination for Ubc13-Ub-RNF4 RING

Data were collected on a Rigaku Saturn 944+ CCD with a Rigaku MM007 HFM generator (wavelength 1.54 Å) at 100 K using 0.25 oscillations for 720 images. Data were indexed, integrated and scaled using XIA2, XDS and CCP4³⁰⁻³⁵. The structure was solved by molecular replacement using PHASER³⁶. Chains D and G are missing due to the absence of Ube2V2. The models were adjusted to fit electron density maps using COOT⁴⁰. Residues H186 and K187 in the first RING domain and residues N185, H186, K187 and R188 from the second RING domain were not clearly visible in the electron density map and were therefore deleted from the model. Crystal packing with Ubc13 (Chain B) and ubiquitin (Chain C) from a symmetry related complex is the likely cause of disorder in these loops. The model was refined using REFMAC5³⁷ and evaluated using MolProbity³⁸. The final statistics are shown in Table 1 and the coordinates and data are available at the RCSB with the accession code 5aiu.

Ubiquitination assay

Ubiquitination assays were carried out as previously described¹². The following components were mixed together and incubated at room temperature: 0.1 μM E1, 2.5 μM Ubc13, 2.5 μM Ube2V2, 0.55 μM RNF4, 5.5 μM Ub~4xSUMO-2 or 4xSUMO-2, 20 μM Ub, 3 mM ATP, 5 mM MgCl₂, 50 mM Tris pH 7.5, 150 mM NaCl, 0.5 mM TCEP, 0.1 % NP40. The reaction was stopped with SDS-PAGE loading buffer and analyzed by SDS-PAGE. Gels were stained with Coomassie Blue. Time points were taken at 0, 2, 5, 10, 20, 40, 60 and 100 min. The zero time point was taken before the addition of ATP. Reactions were also analyzed by western blotting with anti-ubiquitin antibody (Dako).

Lysine discharge assay

Ubc13-Ub thioester linked conjugate was prepared by mixing the following components for 15 min at 37 °C: 120 μM Ubc13, 100 μM Ub, 0.2 μM Ube1, 50 mM Tris pH 7.5, 150 mM NaCl, 3 mM ATP, 5 mM MgCl₂, 0.5 mM TCEP, 0.1 % NP40. Apyrase (4.5 U ml⁻¹, New England BioLabs) was then added to the reaction to deplete the ATP. The thioester was then mixed in a 1:1 ratio with different combinations of RNF4 constructs, Ube2V2 and L-lysine buffered with 50 mM Tris pH 7.5, 150 mM NaCl, 0.1 % NP40, 0.5 mM TCEP. The final concentration of each component is about 50 μM thioester, 150 mM L-lysine, 100 μM Ube2V2 and 0.55 μM RNF4 or 0.275 μM RNF4-RING. The reaction was incubated at room temperature and stopped with non-reducing SDS-PAGE loading buffer and analyzed by SDS-PAGE. Gels were stained with SYPRO Orange (Life Technologies, S6650) and imaged using Bio-Rad gel doc with the SYPRO Ruby filter. The thioester was quantified using Image Lab. Reaction rates were derived from 4 – 6 time points in the linear range of the reaction. Individual reaction rates are shown for duplicate or triplicate reactions as well as the mean reaction rate. Zero time point was taken before the addition of RNF4, Ube2V2 and L-lysine.

ITC experiment

ITC experiments were performed on a MicroCal iTC 200 (GE Healthcare). All proteins were dialyzed overnight into degassed 50 mM Tris pH 7.5, 150 mM NaCl, 0.5 mM TCEP.

Protein concentrations were determined by absorbance at 280 nm and extinction coefficients were predicted using ExPASy ProtParam tool. 250 – 370 μM WT Ube2V2 or Ube2V2 mutants were titrated into 25 – 37 μM WT Ubc13 or Ubc13 mutants. The experiment consisted of one injection of 0.5 μl followed by 1.8 μl injections. The injection speed was set to 1 $\mu\text{l s}^{-1}$ with a 2-minute delay after each injection and the stirring speed was 750 RPM. A blank titration of WT Ube2V2 or Ube2V2 mutants was performed to account for the heat of dilution of Ube2V2 and subtracted from the experimental data. Raw data were analyzed using MicroCal Origin software. Data were fitted using a one-binding site model.

Supplementary Material

Refer to Web version on PubMed Central for supplementary material.

Acknowledgements

We thank M. Alpey for assistance with data collection and the Division of Signal Transduction Therapy, University of Dundee for the gift of His-UBE1. This work was supported by grants from Cancer Research UK (C434/A13067), the Wellcome Trust (098391/Z/12/Z) and Biotechnology and Biological Sciences Research Council (BB/J016004/1). Both 098391/Z/12/Z (R.T.H.) and WT100209MA (J.H.N.) are supported as Senior Investigators of the Wellcome Trust. J.H.N. is supported as a Royal Society Wolfson Merit Award Holder.

References

1. Metzger MB, Pruneda JN, Klevit RE, Weissman AM. RING-type E3 ligases: Master manipulators of E2 ubiquitin-conjugating enzymes and ubiquitination. *Biochimica et Biophysica Acta (BBA) - Molecular Cell Research*. 2014; 1843:47–60. [PubMed: 23747565]
2. Scheffner M, Kumar S. Mammalian HECT ubiquitin-protein ligases: Biological and pathophysiological aspects. *Biochimica et Biophysica Acta (BBA) - Molecular Cell Research*. 2014; 1843:61–74. [PubMed: 23545411]
3. Dou H, Buetow L, Sibbet GJ, Cameron K, Huang DT. BIRC7-E2 ubiquitin conjugate structure reveals the mechanism of ubiquitin transfer by a RING dimer. *Nat. Struct. Mol. Biol*. 2012; 19:876–83. [PubMed: 22902369]
4. Plechanovova A, Jaffray EG, Tatham MH, Naismith JH, Hay RT. Structure of a RING E3 ligase and ubiquitin-loaded E2 primed for catalysis. *Nature*. 2012; 489:115–20. [PubMed: 22842904]
5. Pruneda JN, et al. Structure of an E3:E2-Ub complex reveals an allosteric mechanism shared among RING/U-box ligases. *Mol. Cell*. 2012; 47:933–42. [PubMed: 22885007]
6. Berndsen CE, Wolberger C. New insights into ubiquitin E3 ligase mechanism. *Nat. Struct. Mol. Biol*. 2014; 21:301–307. [PubMed: 24699078]
7. Tatham MH, et al. RNF4 is a poly-SUMO-specific E3 ubiquitin ligase required for arsenic-induced PML degradation. *Nat. Cell Biol*. 2008; 10:538–46. [PubMed: 18408734]
8. Galanty Y, Belotserkovskaya R, Coates J, Jackson SP. RNF4, a SUMO-targeted ubiquitin E3 ligase, promotes DNA double-strand break repair. *Genes Dev*. 2012; 26:1179–1195. [PubMed: 22661229]
9. Guzzo CM, et al. RNF4-Dependent Hybrid SUMO-Ubiquitin Chains are Signals for RAP80 and thereby Mediate the Recruitment of BRCA1 to Sites of DNA Damage. *Science Signaling*. 2012; 5:ra88–ra88. [PubMed: 23211528]
10. Vyas R, et al. RNF4 is required for DNA double-strand break repair in vivo. *Cell Death and Differentiation*. 2013; 20:490–502. [PubMed: 23197296]
11. Yin Y, et al. SUMO-targeted ubiquitin E3 ligase RNF4 is required for the response of human cells to DNA damage. *Genes Dev*. 2012; 26:1196–208. [PubMed: 22661230]
12. Rojas-Fernandez A, et al. SUMO chain-induced dimerization activates RNF4. *Mol. Cell*. 2014; 53:880–92. [PubMed: 24656128]

13. Hofmann RM, Pickart CM. Noncanonical MMS2-Encoded Ubiquitin-Conjugating Enzyme Functions in Assembly of Novel Polyubiquitin Chains for DNA Repair. *Cell*. 1999; 96:645–653. [PubMed: 10089880]
14. Eddins MJ, Carlile CM, Gomez KM, Pickart CM, Wolberger C. Mms2-Ubc13 covalently bound to ubiquitin reveals the structural basis of linkage-specific polyubiquitin chain formation. *Nat. Struct. Mol. Biol.* 2006; 13:915–20. [PubMed: 16980971]
15. Tatham MH, Plechanovova A, Jaffray EG, Salmen H, Hay RT. Ube2W conjugates ubiquitin to alpha-amino groups of protein N-termini. *Biochem. J.* 2013; 453:137–45. [PubMed: 23560854]
16. Lewis MJ, Saltibus LF, Hau DD, Xiao W, Spyropoulos L. Structural basis for non-covalent interaction between ubiquitin and the ubiquitin conjugating enzyme variant human MMS2. *J. Biomol. NMR.* 2006; 34:89–100. [PubMed: 16518696]
17. McKenna S, et al. Energetics and specificity of interactions within Ub.Uev.Ubc13 human ubiquitin conjugation complexes. *Biochemistry.* 2003; 42:7922–30. [PubMed: 12834344]
18. McKenna S, et al. Noncovalent interaction between ubiquitin and the human DNA repair protein Mms2 is required for Ubc13-mediated polyubiquitination. *J. Biol. Chem.* 2001; 276:40120–6. [PubMed: 11504715]
19. Moraes TF, et al. Crystal structure of the human ubiquitin conjugating enzyme complex, hMms2-hUbc13. *Nat. Struct. Biol.* 2001; 8:669–73. [PubMed: 11473255]
20. Spyropoulos L, Lewis MJ, Saltibus LF. Main chain and side chain dynamics of the ubiquitin conjugating enzyme variant human Mms2 in the free and ubiquitin-bound States. *Biochemistry.* 2005; 44:8770–81. [PubMed: 15952783]
21. VanDemark AP, Hofmann RM, Tsui C, Pickart CM, Wolberger C. Molecular insights into polyubiquitin chain assembly: crystal structure of the Mms2/Ubc13 heterodimer. *Cell.* 2001; 105:711–20. [PubMed: 11440714]
22. Zhang M, et al. Chaperoned ubiquitylation--crystal structures of the CHIP U box E3 ubiquitin ligase and a CHIP-Ubc13-Uev1a complex. *Mol. Cell.* 2005; 20:525–38. [PubMed: 16307917]
23. Reverter D, Lima CD. Insights into E3 ligase activity revealed by a SUMO-RanGAP1-Ubc9-Nup358 complex. *Nature.* 2005; 435:687–92. [PubMed: 15931224]
24. Scott DC, et al. Structure of a RING E3 trapped in action reveals ligation mechanism for the ubiquitin-like protein NEDD8. *Cell.* 2014; 157:1671–84. [PubMed: 24949976]
25. Yunus AA, Lima CD. Lysine activation and functional analysis of E2-mediated conjugation in the SUMO pathway. *Nat. Struct. Mol. Biol.* 2006; 13:491–499. [PubMed: 16732283]
26. Berndsen CE, Wiener R, Yu IW, Ringel AE, Wolberger C. A conserved asparagine has a structural role in ubiquitin-conjugating enzymes. *Nat. Chem. Biol.* 2013; 9:154–6. [PubMed: 23292652]
27. Wu PY, et al. A conserved catalytic residue in the ubiquitin-conjugating enzyme family. *EMBO J.* 2003; 22:5241–50. [PubMed: 14517261]
28. Chang L, Zhang Z, Yang J, McLaughlin SH, Barford D. Molecular architecture and mechanism of the anaphase-promoting complex. *Nature.* 2014; 513:388–393. [PubMed: 25043029]
29. Plechanovova A, et al. Mechanism of ubiquitylation by dimeric RING ligase RNF4. *Nat. Struct. Mol. Biol.* 2011; 18:1052–9. [PubMed: 21857666]
30. Collaborative Computational Project, N. The CCP4 suite: programs for protein crystallography. *Acta Crystallogr. D Biol. Crystallogr.* 1994; 50:760–3. [PubMed: 15299374]
31. Evans P. Scaling and assessment of data quality. *Acta Crystallogr. D Biol. Crystallogr.* 2006; 62:72–82. [PubMed: 16369096]
32. Evans PR. Scaling of MAD Data. *Proceedings of CCP4 Study Weekend.* 1997
33. Kabsch W. Xds. *Acta Crystallogr. D Biol. Crystallogr.* 2010; 66:125–32. [PubMed: 20124692]
34. Winn MD, et al. Overview of the CCP4 suite and current developments. *Acta Crystallogr. D Biol. Crystallogr.* 2011; 67:235–42. [PubMed: 21460441]
35. Winter G. xia2: an expert system for macromolecular crystallography data reduction. *J. Appl. Crystallogr.* 2010; 43:186–190.
36. McCoy AJ, et al. Phaser crystallographic software. *J Appl. Crystallogr.* 2007; 40:658–674. [PubMed: 19461840]

37. Murshudov GN, Vagin AA, Dodson EJ. Refinement of macromolecular structures by the maximum-likelihood method. *Acta Crystallogr. D Biol. Crystallogr.* 1997; 53:240–55. [PubMed: 15299926]
38. Chen VB, et al. MolProbity: all-atom structure validation for macromolecular crystallography. *Acta Crystallogr. D Biol. Crystallogr.* 2010; 66:12–21. [PubMed: 20057044]
39. Krissinel E, Henrick K. Inference of Macromolecular Assemblies from Crystalline State. *J. Mol. Biol.* 2007; 372:774–797. [PubMed: 17681537]
40. Emsley P, Lohkamp B, Scott WG, Cowtan K. Features and development of Coot. *Acta Crystallographica Section D.* 2010; 66:486–501. [PubMed: 20383002]

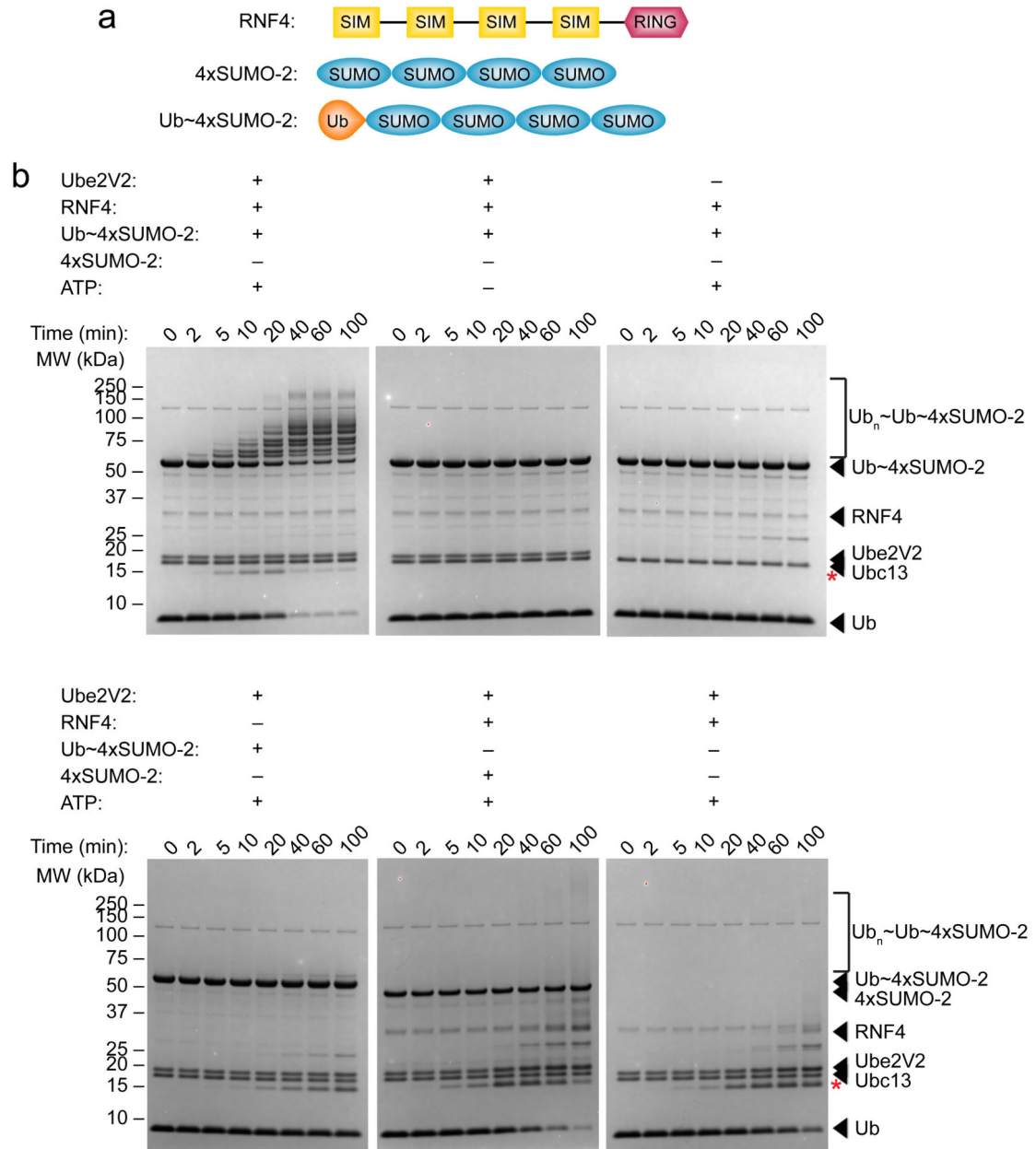


Figure 1. Biochemical analysis of RNF4 catalysed K63 linked polyubiquitination by Ube2V2–Ubc13 complex

(a) Cartoon representation of RNF4, 4xSUMO-2, and Ub~4xSUMO-2. RNF4 contains four N-terminal SIMs (yellow) followed by a C-terminal RING domain (dark pink). 4xSUMO-2 contains four linearly fused SUMO-2 molecules (blue). Ub~4xSUMO-2 has a ubiquitin molecule (orange) linearly fused to the N-terminus of 4xSUMO-2.

(b) Coomassie-blue stained SDS-PAGE analysis of ubiquitination assays containing various combinations of Ube2V2, RNF4, Ub~4xSUMO-2, 4xSUMO-2 and ATP. Time points are denoted above the gels. The red asterisk indicates formation of di-ubiquitin.

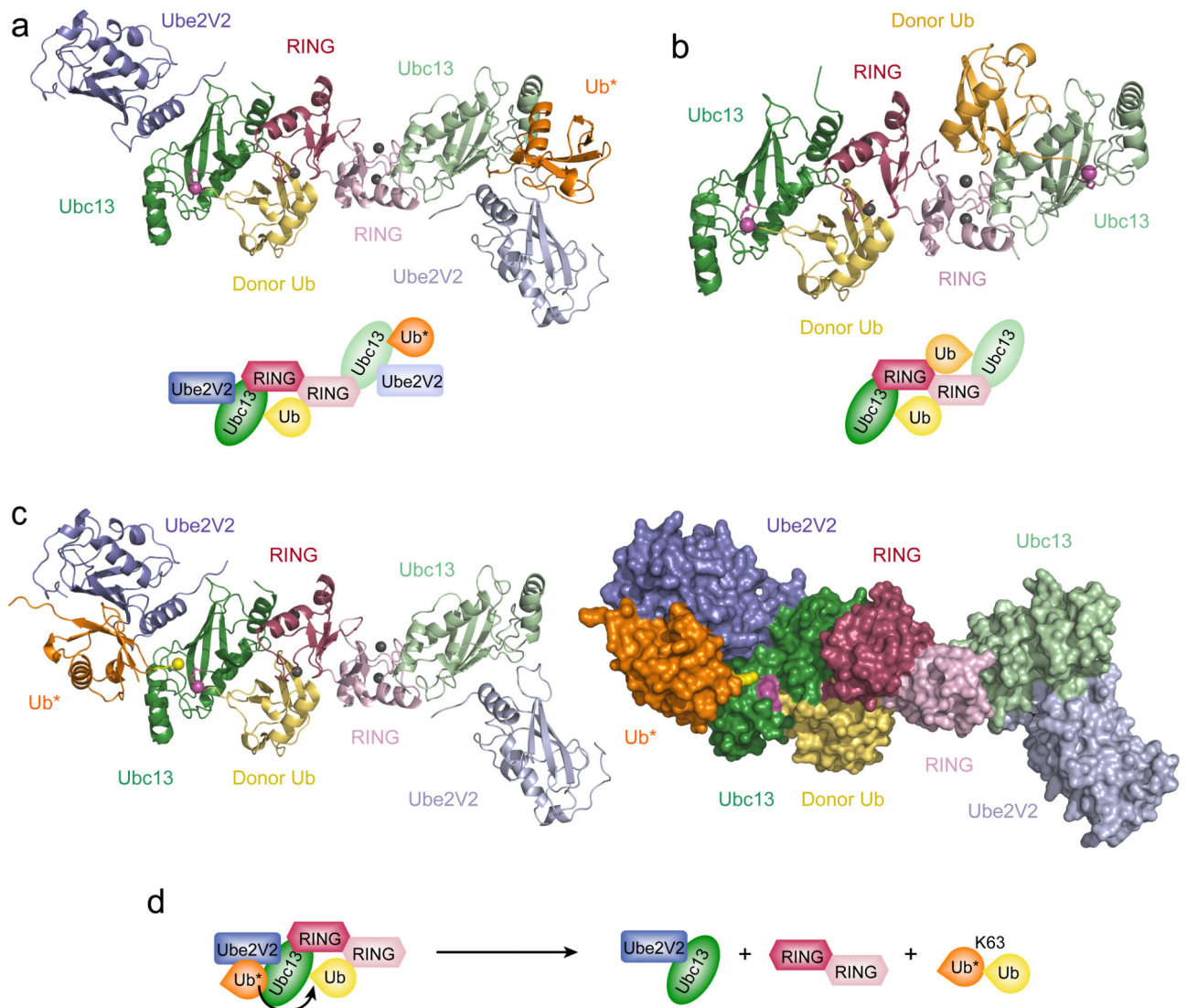


Figure 2. Structure of ubiquitin loaded Ubc13 in complex with Ube2V2 and the RING domain of RNF4 showing specificity for K63 linked polyubiquitination

(a) Ribbon (top) and cartoon (bottom) representation of Ube2V2 (dark and pale blue) and the linearly fused RING domain dimer of RNF4 (dark and pale pink) in complex with ubiquitin loaded Ubc13. Ubc13 is shown in dark and pale green while the donor ubiquitin is yellow and Ub* is coloured orange. Ubc13 K87 and donor ubiquitin G76 are highlighted in magenta with the isopeptide linkage highlighted with a magenta sphere. Zn ions are shown as grey spheres.

(b) Ribbon (top) and cartoon (bottom) representation of the ubiquitin-loaded Ubc13 in complex with the RING domain of RNF4. The colour scheme is the same as in **a** and the second donor ubiquitin is light orange.

(c) Ribbon (left) and surface (right) representation of the same complex as in **a** where Ub* has been transformed in order to generate the canonical model. The colour scheme is the

same as in **a**. Ub* K63 is coloured in yellow with the ϵ -amine highlighted with a yellow sphere.

(d) Cartoon diagram of K63 linked chain formation based on the Ubc13~Ub– Ube2V2– RNF4 RING structure.

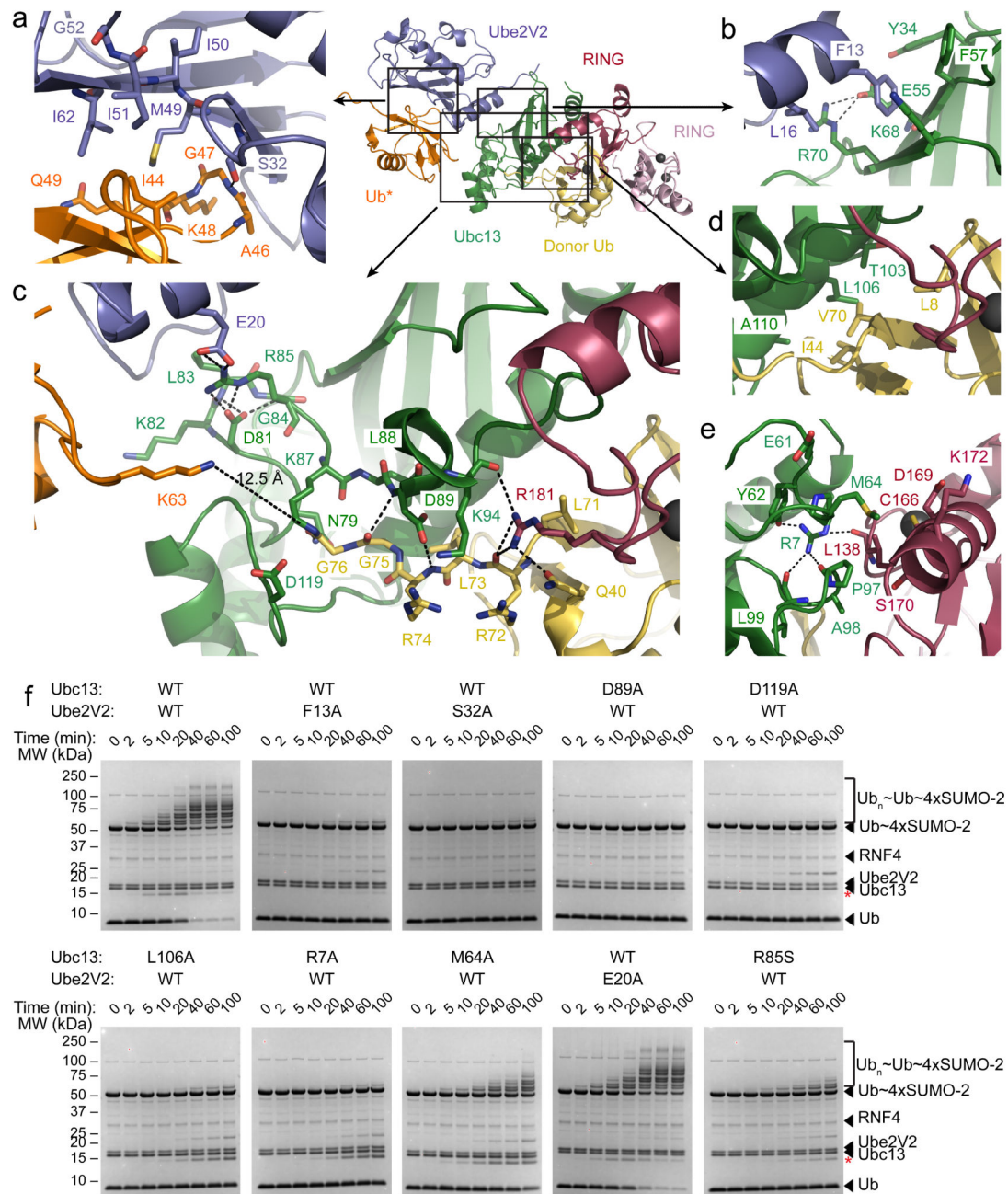


Figure 3. Mutational analysis of the Ubc13~Ub-Ube2V2-RNF4 RING complex

(a) Detailed molecular interface between Ub* (orange) and Ube2V2 (blue) from the canonical model.

(b) Detail of the hydrophobic pocket in Ubc13 (green) for Ube2V2 (blue).

(c) Interaction between the C-terminal tail of the donor ubiquitin (yellow) and the active site groove of Ubc13 (green). K63 of Ub* (orange) is shown and the distance between its ϵ -amino group and the carbonyl carbon of the donor ubiquitin G76 is indicated. Interactions between the D81 to R85 loop of Ubc13 and Ube2V2 (blue) are also shown.

- (d) The hydrophobic interface between Ubc13 (green) and ubiquitin (yellow) in the Ubc13~Ub conjugate bound to the RING domain of RNF4.
- (e) Molecular detail of the interaction surface between Ubc13 (green) and the RING domain of RNF4 (dark pink).
- (f) Coomassie-blue stained SDS-PAGE analysis of ubiquitination assays containing wild type (WT) or mutants of Ubc13 and Ube2V2. The red asterisk indicates formation of di-ubiquitin.

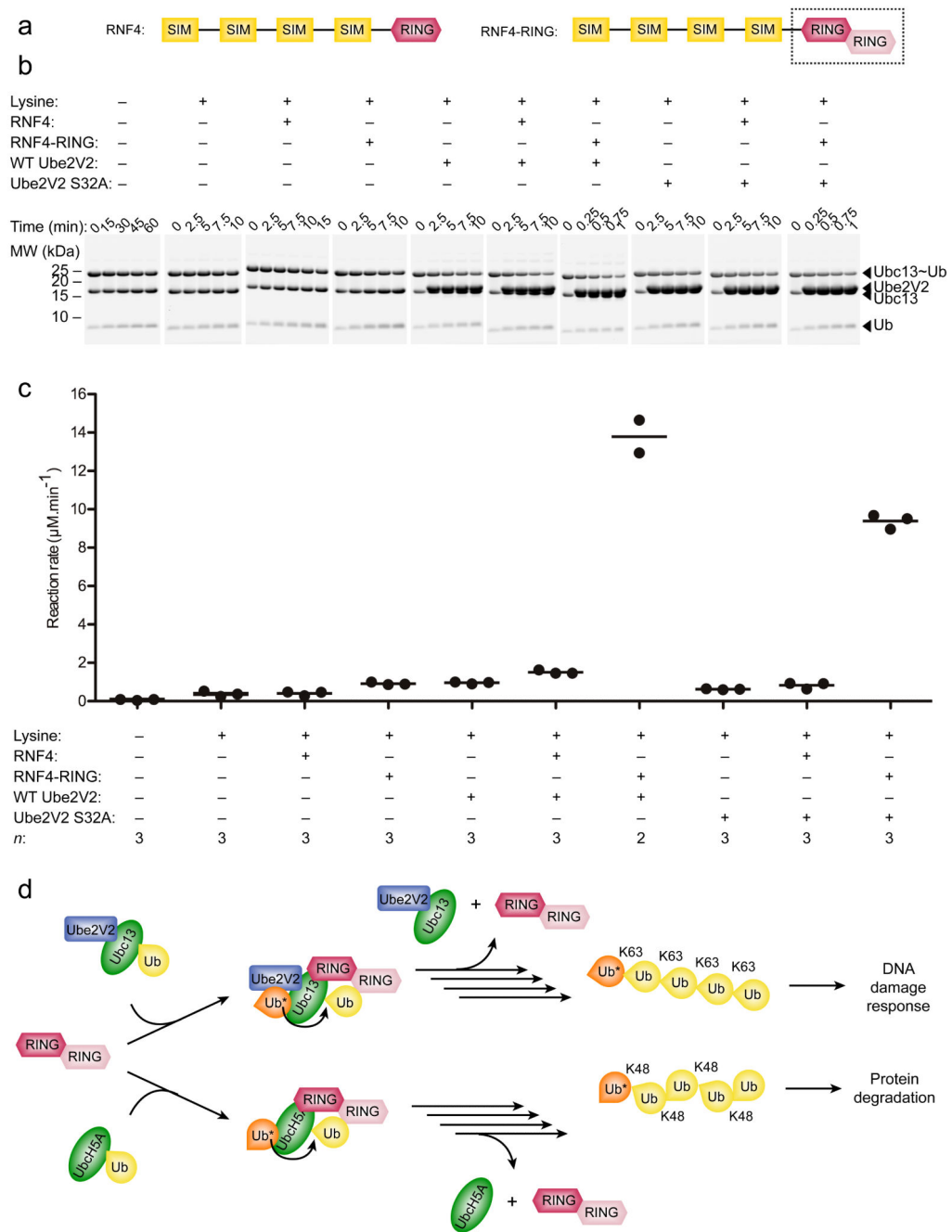


Figure 4. Both Ube2V2 and dimeric RNF4 are required for activation of the Ubc13-Ub thioester conjugate

(a) Cartoon representation of RNF4 and RNF4-RING. RNF4-RING has a second RING domain of RNF4 (pale pink) linearly fused to RNF4. The RING domain dimer, which was used in crystallography, is highlighted with a black dotted line.

(b) SYPRO orange stained SDS-PAGE analysis of lysine discharge assays in the presence of RNF4, RNF4-RING, WT Ube2V2 and Ube2V2 S32A. Time points are denoted above each gel. Uncropped gels are available in Supplementary Data Set 1.

(c) Reaction rates were obtained for lysine discharge assays shown in **b**. The reaction rates from two or three technical replicates are shown as black dots and the mean reaction rates are shown as black horizontal bars. Number of replicates (n) is denoted below the graph. Spreadsheet containing reaction rate calculations are available in Supplementary Data Set 2.

(d) Schematic diagram of RNF4 catalysing the formation of K63 and K48 linked polyubiquitin chains in complex with Ube2V2–Ubc13 and UbcH5A respectively.

Table 1

Data collection and refinement statistics (molecular replacement)

	RING-Ubc13-Ub-Ube2V2	RING-Ubc13-Ub
Data collection		
Space group	P3 ₂ 21	P2 ₁ 2 ₁ 2
Cell dimensions		
<i>a</i> , <i>b</i> , <i>c</i> (Å)	77.5, 77.5, 328.4	69.2, 169.2, 52.6
α , β , γ (°)	90.00, 90.00, 120.00	90.00, 90.00, 90.00
Resolution (Å)	67 - 3.4(3.49-3.40) ^a	32 - 2.21(2.26 - 2.21)
<i>R</i> _{merge}	3.4(62.9)	6.2 (15.3)
<i>I</i> / σ <i>I</i>	25.7(1.9)	20.9(7.8)
Completeness (%)	88.9(98.3)	95.0(74.8)
Redundancy	4.1(3.4)	5.7(3.7)
Refinement		
Resolution (Å)	67 - 3.4	32 - 2.21
No. reflections	14,864	30,359
<i>R</i> _{work} / <i>R</i> _{free}	0.208 / 0.286	21.7 / 25.5
No. atoms		
Protein	6738	4524
Zn ²⁺	4	4
Ethylene glycol	0	24 (6 molecules)
Water	0	33
<i>B</i> factors		
Protein	140	25
Zn ²⁺	117	17
Ethylene glycol	-	19
Water	-	18
r.m.s. deviations		
Bond lengths (Å)	0.014	0.014
Bond angles (°)	1.6	1.7

One crystal per structure.

^aValues in parentheses are for highest-resolution shell.